

**Southern University and A&M College 2008-2011 Final Technical Report  
Department of Mechanical Engineering  
Baton Rouge, LA 70813**

**A Study of Advanced Materials for Gas Turbine Coatings at Elevated Temperatures Using  
Selected Microstructures and Characteristic Environments for Syngas Combustion**

**FINAL TECHNICAL REPORT**

**February 11, 2008- February 10, 2011**

**Principal Investigator:**

Dr. Ravinder M. Diwan  
Professor, Department of Mechanical Engineering  
Southern University and A&M College  
Baton Rouge, LA 70813  
Phone: (225)771-2073 FAX: (225) 771-4877

**DOE NETL Final Technical report**

**DE-FG-26-08NT001471**

**Department of Mechanical Engineering  
Southern University and A&M College  
Baton Rouge, LA 70813**

**Principal Investigator:**

Dr. Ravinder M. Diwan, Professor  
Department of Mechanical Engineering  
Southern University and A & M College  
Baton Rouge, LA 70813  
Phone: (225)771-2073 FAX: (225) 771-4877  
Email: [diwan@engr.subr.edu](mailto:diwan@engr.subr.edu)

**Faculty-Co-Principal Investigators:**

Dr. Patrick F. Mensah, Professor  
Dr. Guoqiang Li, Associate Professor  
  
Department of Mechanical Engineering  
Southern University and A & M College  
Baton Rouge, LA 70813

**Post Doc/Research Associates:**

Ms. Nalini Uppu  
Dr. Stephen Akwaboa

**Graduate Students:**

Ms. Monica B. Silva  
Mr. Ebubekir Beyazoglu  
Mr. Ogad Agu  
Mr. Naresh Polasa

**Undergraduate Students:**

Mr. Lawrence Bazille

**Subcontractors/ Co-Investigators:**

Dr. Douglas E. Wolfe, Assistant Professor  
Department of Materials Science and Engineering  
Advanced Coatings Department Head  
Applied Research Laboratory  
The Pennsylvania State University, University Park, PA 16802

Dr. Purush Sahoo, Materials Solutions International Inc  
2643 Williams Grant St., Sugarland, TX 77479

## **DISCLAIMER**

**This report was prepared as an account of the work sponsored by an agency of the United States Government. Neither the United States Government nor any agency thereof, nor any of their employees, makes any warranty, express or implied, or assumes any legal liability or responsibility for the accuracy, completeness, or usefulness of any information, apparatus, product, or process disclosed, or represents that its use would not infringe privately owned rights. Reference herein to any specific commercial product, process or service by trade name, trademark or manufacturer, or otherwise does not necessarily constitute or imply its endorsement, recommendation, or favoring by the United States Government or any agency thereof. The views and opinions of authors expressed herein do not necessarily state or reflect those of the United States Government or any agency thereof.**

## ABSTRACT

Thermal barrier coatings (TBCs) that can be suitable for use in industrial gas turbine engines have been processed and compared with electron beam physical vapor deposition (EBPVD) microstructures for applications in advanced gas turbines that use coal-derived synthesis gas. Thermo-physical properties have been evaluated of the processed air plasma sprayed TBCs with standard APS-STD and vertically cracked APS-VC coatings samples up to 1300°C. Porosity of these selected coatings with related microstructural effects have been analyzed in this study. Wet and dry thermal cycling studies at 1125°C and spalling resistance thermal cycling studies to 1200°C have also been carried out. Type I and Type II hot corrosion tests were carried out to investigate the effects of microstructure variations and additions of alumina in YSZ top coats in multi-layered TBC structures. The thermal modeling of turbine blade has also been carried out that gives the capability to predict in-service performance temperature gradients. In addition to isothermal high temperature oxidation kinetics analysis in YSZ thermal barrier coatings of NiCoCrAlY bond coats with 0.25% Hf. This can affect the failure behavior depending on the control of the thermally grown oxide (TGO) growth at the interface. The TGO growth kinetics is seen to be parabolic and the activation energies correspond to interfacial growth kinetics that is controlled by the diffusion of O<sub>2</sub> in Al<sub>2</sub>O<sub>3</sub>. The difference between oxidation behavior of the VC and STD structures are attributed to the effects of microstructure morphology and porosity on oxygen ingress into the zirconia and TGO layers. The isothermal oxidation resistance of the STD and VC microstructures is similar at temperatures up to 1200°C. However, the generally thicker TGO layer thicknesses and the slightly faster oxidation rates in the VC microstructures are attributed to the increased ingress of oxygen through the grain boundaries of the vertically cracked microstructures. The plasma sprayed TBC microstructure (VC and STD) with NiCoCrAlY–Hf bond coat are stable up to 1100°C. However, as with other TBC structures, a considerable amount of interdiffusion was observed in the different layers, although the TBC growth was self-limiting and parabolic. The addition of Hf to the VC microstructure appears to have some potential for the future development of robust TBCs with improved isothermal and service temperatures in advanced gas turbines.

## TABLE OF CONTENTS

Disclaimer	iii
Abstract	iv
1. Executive Summary	3
2. Project Description	4
3. Experimental Approach and Methods	5
4. Results and Discussion	13
5. Key Outcomes	25
6. Conclusions	26
7. References	28

DOE Award Number: DE-FG-26-08NT001471  
Type of Report: Final Technical Report  
Reporting Period: Feb. 11, 2008 - Feb.10, 2011  
Name of Submitting Organization: Southern University

Name, Phone Number and Fax Number of Preparer: Dr. Ravinder M. Diwan  
Phone: 225-771-2073  
Fax: 225-771-4877

## FINAL TECHNICAL REPORT

### **A Study of Advanced Materials for Gas Turbine Coatings at Elevated Temperatures Using Selected Microstructures and Characteristic Environments for Syngas Combustion**

Prepared for:  
Dr. Richard J. Dunst  
DOE Project Officer  
National Energy Technology Laboratory  
626 Cochrans Mill Road, PO Box 10940  
Pittsburgh, PA 15236-0940

Ms. Mary Beth Jackline-Pearse  
DOE Award Administrator  
National Energy Technology Laboratory  
626 Cochrans Mill Road, PO Box 10940  
Pittsburgh, PA 15236-0940

Principal Investigator:  
Dr. Ravinder M. Diwan, Professor  
Department of Mechanical Engineering  
Southern University and A&M College  
Baton Rouge, LA 70813  
Phone: 225-771-2073  
Fax: 225-771-4877  
Email: [diwan@engr.subr.edu](mailto:diwan@engr.subr.edu)

## 1. EXECUTIVE SUMMARY

The overall objective of this research project has been to study the effects of the air plasma spray (APS) coated microstructures for making thermal barrier coatings (TBCs) that are suitable for use in industrial gas turbine engines and compare these with electron beam physical vapor deposition (EBPVD) microstructures for applications in advanced gas turbines that use coal derived synthesis gas. The research work reported here is for this referenced grant for a period of three years starting from February 11, 2008 to February 10, 2011. The goal for this research has focused on the development of APS test samples with standard splat and vertical columnar structures and EBPVD specimens that have been used for thermal properties characterization. In addition, some multilayered specimens with YSZ including alumina formulations have been also processed and tested for elevated temperature and corrosion effects. Specifically, the various tasks of the project have been carried out to meet the project milestones for the three years of the research project as per the following milestones as indicated below:

### Year 1

Milestone 1.1 Develop APS and EBPVD test samples with optimal processing parameters

Milestone 1.2 Benchmark thermo-physical properties experimental testing of APS processed and EBPVD TBCs.

### Year 2

Milestone 2.1: Experimental hot corrosion testing in sulfur environment of developed TBCs in synthesis gas environment and thermal cycling oxidation testing in dry and moisture environments. Multilayered APS TBCs and EBPVD microstructure processing and evaluations of samples.

Milestone 2.2: Thermo-physical properties and thermo-mechanical behavior and spalling studies.

### Year 3

Milestone 3.1: Studies of structural and thermo physical properties of TBCs including alumina based TBCs and comparative thermal cycling and spalling studies of TBCs

Milestone 3.2: Development of performance models to predict the lives of developed TBCs in this study.

In the first year of the project, we developed APS and EBPVD test samples with optimal processing parameters that were used for thermo-physical properties characterizations at elevated temperatures. These were investigated for specific IN 738 superalloy materials for substrate specimen preparation, and bond coats of NiCoCrAlY, and top coats of selected thickness of YSZ TBC. Earlier studies of processed standard and vertically cracked APS samples were used for spalling resistance and thermal cycling at 1250 and 1350 ° C; however these showed poor response due to feeble development of vertically cracked microstructures. Later specimens were prepared using a bond coat of NiCoCrAlY powder with 0.25% Hf recommended that could provide specimens with better performance of the APS coatings both for standard and vertically

cracked VC microstructured specimens. These bond coated specimens were then used to produce top coatings of 300 and 600 microns thickness for both standard and VC microstructured specimens and these bond coated specimens were used to process 300 micron thickness EBPVD top coatings, and these were analyzed for microstructures and their oxidation behavior and thermal characteristics at Southern University. Work on selected test specimens for evaluating dry and wet oxidation performance at Applied Research Laboratory at PSU was also started as per our test plans at 1125 ° C. Thermo-physical properties and microstructure effects were characterized using our laser Flashline 5000 equipment at Advanced Materials Research Laboratory at Southern University. The optimal processing of samples was carried out and also benchmark thermo-physical properties of APS processed and EBPVD TBCs were tested.

In the second year, developed TBC samples were tested for dry and wet oxidation cycling studies at 1125 ° C and work was carried out in line with milestone goals of this year to conduct experimental hot corrosion testing in sulfur environment of developed TBCs in synthesis gas environment and thermal cycling oxidation testing in dry and moisture environments. Multilayered APS TBCs and EBPVD microstructure processing and evaluations of samples and thermo-physical properties and thermo-mechanical behavior and spalling studies were also carried out. Work was continued on the development of multi-sectioned TBCs to form structure of high strain tolerance and thermal conductivity. Hot corrosion studies of Type I and Type II were carried out of selected TBC test samples.

In the third year, work was carried out to completion as per milestones related to porosity and microstructural effects on selected processed TBC samples and comparative analysis of thermal cycling and spalling behavior of the TBCs in effort to develop performance model including effects of thermal radiation on APS coated GT blade and analysis of isothermal interfacial kinetics of oxidation.

During the period of this award, the work resulted in several refereed publications and conference presentations. Details of all these are included in this report.

## **2. PROJECT DESCRIPTION**

Advanced Materials for Gas Turbine Coatings using selected microstructured regimes for use at Elevated Temperatures and Characteristic Environments for Syngas Combustion in high temperature conditions to 1300 ° C have been investigated. This is of critical interest to enhance the thermo-physical properties of advanced air plasma sprayed TBCs on NiCoCrAlY bond coats on superalloy substrate materials such as IN 738 using state of the art YSZ top coats of controlled microstructures. Several investigators have looked into behavior of YSZ coatings and evaluations of such TBC materials [1-6] and the goals of such studies have been to extend the envelope of applications for such materials for increasing efficiencies of materials at elevated temperatures and under hot corrosion test conditions. In our studies, one of the major issues has been to understand effects of splat (lamellar) horizontal standard APS microstructures and of vertically cracked VC microstructures processed by APS methods or electron beam physical deposition EB-PVD coated microstructures. Role of thermal conductivity and physical properties such as affects of porosity and microstructures has been analyzed, including multi-layered YSZ coatings with inclusion of alumina in the top coat microstructures.



This three year project has been geared to develop TBC samples using APS and EB-PVD methods and these have been evaluated for porosity, thermal properties and thermal cycling and wet and dry oxidation studies. Also, thermal cycling behavior and hot corrosion effects have been analyzed at elevated temperatures and in the final year efforts have been made to understand the role of thermal oxidation to reduce spalling effects under typical hot component operating conditions. A new bond coat formulation using NiCoCrAlY with 0.25% Hf had provided better properties and failure resistance of processed TBCs and this has been used in the coated microstructures carried out. Also, multilayered structures have been analyzed using top coats of YSZ and Al<sub>2</sub>O<sub>3</sub>. The modeling of oxidation kinetics has been carried out for high temperature conditions up to 1200 ° C. Previously, some studies have indicated possible beneficial effects of columnar vertically cracked VC microstructures and these have been evaluated in VC APS and EB-PVD structures. Thermal modeling has been attempted to reduce thermal losses in TBC coated microstructures for applications in turbine blades. As part of this project, three graduate students completed their Master's thesis at Southern University and one graduate student completed Ph.D. as part of this research work. Also, two research associates have carried out research on this project. As part of this research several research publications have been accomplished that are listed and included in this report separately.

### **3. EXPERIMENTAL APPROACH AND METHODS**

Thermal barrier coatings have been applied on gas turbine hot section components for more than four decades, but there are still many challenging problems facing the development of a robust TBC. The reliability of thermal barrier coatings is determined by the composition of the coating and their mechanical and thermal properties. Atmospheric plasma spray (APS) and electron beam physical vapor deposition (EBPVD) are two methods commonly used in industry to make the TBCs. A typical TBC system is comprised of three layers: bond coat, thermally grown oxide, and the ceramic coating; all three applied on top of the gas turbine engine metallic components.

#### **3.1 Specimen Preparation**

Air Plasma Spray methods and Electron Beam-Physical Vapor Deposition EB-PVD methods were used to fabricate TBC samples on EDM machined inconel IN 738 substrate discs with selected bond coats and top coats of about 7.65 wt % yttria stabilized zirconia YSZ materials suitable for thermo-physical properties and other characterizations. Earlier vintage of specimens had used bond coats of NiCoCrAlY bond coats that were then replaced with better performance bond coats of Sulzer Metco powder 386 of nominal composition Ni-22Co-17Cr-12.5Al-0.25Hf-0.4Si-0.6Y (weight %). This later formulation bond coating with 0.25% Hf had provided better spalling resistance and was recommended and was used for both the standard (APS-STD) and the vertically cracked (APS-VC) samples and for EPBVD samples.

### 3.1.1 APS Microstructured Specimens

During plasma spray process the combination of different process parameters will lead to a distinct and unique microstructure. Typically, APS coatings have a lamellae structure composed of multiple layers; the advantage of this standard APS STD structure is to produce a low thermal conductivity coating to provide a thermal barrier effect, but this structure tends to fail by spallation compared to the so called vertically cracked structure. The vertically cracked structure is obtained by modifying the plasma spray process parameters. Several patents have been developed in order to produce the vertically cracked APS VC structure. It has been reported by Grey et. al. [1] that the columnar grain growth could be promoted by increasing the deposition surface temperature from 600 °C to 950 °C during plasma spray process, an increasing degree of columnarity was found in the TBCs, which improved spallation resistance of the TBCs.

Gas turbines engine components undergo severe thermal and mechanical loads during operation, thus the lifetime of the TBC systems are limited by thermal-mechanical fatigue. There are several failure mechanisms of TBCs, typically failure by spallation [2, 3]. To study the failure mechanism, thermal cycling tests are usually performed to evaluate the behavior of the TBCs. During these tests, thermal barrier coating samples can be heated by electrical furnace to a controlled temperature for a certain period of time. The adhesive failure is due to fractures between the coating and the substrate, and the cohesive failure is due to the fractures within the coatings. A study reported that the adhesion strength of APS coatings (made of YSZ on a steel substrate without bond coat) was reduced by 25% after heat treatment at 1150 °C for 10 h [4]. The use of different bond coat compositions leads to different modes of failures. For example, the use of NiCr(19%)Al(6%) results in a fracture in the interface between the top coat and the bond coat, which is an adhesive type of failure [5]. On the other hand the addition of chromium and aluminum increases the total coating lifetime [6]. In addition to increasing the lifetime, a NiCoCrAlY bond coat aids the TGO formation which is in direct contact with the superalloy substrate improving the bonding to the substrate [7]. The degradation in bond strength and the difference between the coefficients of thermal expansions between the bond coat and the ceramic coat promote the coating failure.

In addition, thermal cycling failures of TBC systems have been studied and reported substantially by many researchers. Bartlett et. al [8] reported that failure usually initiated at the bond coat/TBC interface region, but close to the interface with the TGO. In the case of EPBVD coatings, it has been reported that the coating usually fails by cracking along the TGO/bond coat interface [9, 10, 11]. Some studies [12] have reported that for thin top coats (<250 microns in thickness), local separation occurs within the ceramic coating near the TGO/Top coat interface. The driving force for spallation remained a combination of cyclic thermal strain coefficient of thermal expansion mismatch, bond coat oxidation (TGO growth) and cyclic mechanical strain. The failure sequence in the foregoing report indicated that the spallation began with formation of subcritical cracks in the ceramic at < 25% of the exposure life, followed by progressive link-up of such cracks which eventually resulted in dominant in-plane crack within the ceramic near the bond coat-ceramic interface. It is the separation of

ceramic at the dominant crack leads to failure. Thicker coatings ( $\gg 250\mu\text{m}$ ) are reported to fail generally within the ceramic layer but away from the interface.

In our research work, processing of APS top coats of standard and vertically cracked microstructured samples was carried out using Sulzer-Metco plasma torch equipment by Materials Solutions International, MSI, TX. The specimens with bond coats of about  $120\mu\text{m}$  thickness were then applied top coating of about 7.65 wt % Yttria stabilized zirconia YSZ powder to produce standard and vertically cracked microstructured samples. The samples were sprayed using a SG-100 air plasma spray gun with internal powder feed injection. The samples were sprayed using a FANUC 710i robot for precise gun-to-part motion and for repeatability of process. The plasma spray process took about 5 – 8 passes to form the sample depending on the operation parameters, such as speed, powder feed rate, etc. The thicker coating needed a higher processing time because of the extra passes of hot plasma jet. In comparison to STD samples, VC samples needed extra heating to the coating substrates before plasma spray to promote columnar grain growth in-situ.

The samples were sprayed on superalloy inconel IN 738 disks. The diameter and thickness of the substrate disks were 12.54 mm and 3 mm respectively. The samples were tumbled prior to application of bond coat to ensure smoothness of the bond coat/TGO interface. Earlier bond coats were of NiCoCrAlY composition; and later specimens used bond coats of a standard powder Sulzer Metco powder 386 of nominal composition Ni-22Co-17Cr-12.5Al-0.25Hf-0.4Si-0.6Y (weight %). This bond coating had provided better spalling resistance and was recommended and used for both the standard (APS-STD) and the vertically cracked (APS-VC) samples and for EB-PVD samples.

The top coat of the TBC specimens had used 7.65wt%  $\text{Y}_2\text{O}_3$ -  $\text{ZrO}_2$  powders. For the top coat formulations, different procedures and spray parameters were used to form the distinct standard lamellar and the vertically cracked micro structures in the ceramic top coat. In the present study, TBC systems were investigated using NiCoCrAlYHf bond coats with YSZ TBC top coatings of  $300\mu\text{m}$  and  $600\mu\text{m}$  for both standard and VC APS TBC and  $300\mu\text{m}$  thick EB-PVD YSZ top coatings to determine the effect of coating thickness and tailored microstructure in dry and wet thermal cyclic oxidation studies at elevated temperatures, and their thermo-physical properties were characterized along with porosity and microstructural effects.

For study of multi-layered TBC specimens and to analyze effects of alumina in the APS top coated microstructures, test specimen formulations of multi-layered APS TBCs with a standard YSZ dense bottom layer and variations of YSZ and alumina composite top coat layer with 15-50 % alumina were processed and these were used for studies of their characterization and performance behavior. In these test specimens with 300 microns YSZ thickness some specimens were processed with a composite top coat of APS standard YSZ dense bottom layer about 150 microns and YSZ with 15%, 30% and 50% top alumina layer of about 150 microns that were produced for porosity measurements and thermal properties characterizations and performance testing of these under Type I and Type II hot corrosion testing of these along with standard and VC processed YSZ top coats specimens to see the effects of these.

### 3.1.2 EB-PVD Microstructured Specimens

The EB-PVD samples were prepared at Pennsylvania State University by Dr Wolfe, by first tumbling some of the IN738 disks to smoothen its circumference and then applying the bond coat. The bond coated substrates were then processed with TBC using the same equipment and similar EBPVD process as per Wolfe et al [13]. The EB-PVD TBC test specimens were produced using IN 738 superalloy substrate disc specimens that were EDM machined and tumbled as done for processing of APS test specimens for comparative studies of these, of 12.54 mm dia x 3mm thickness. All test specimens were bond coated with NiCoCrAlY doped with 0.25w% Hf of about 125 microns thickness. The bond coated specimens were then EBPVD coated, and the coatings were given YSZ coatings of about 300 microns thickness and these were tested in comparison with the APS specimens produced of similar 300 microns thickness and 600 micron thickness by Materials Solutions International MSI Inc, TX. for comparative wet and dry thermal cycling oxidation testing of the TBC test specimens and other thermo-physical properties characterizations and microstructural effects.

Typical microstructures of the coated TBC specimens of the columnar EB-PVD structure and of the standard and vertically cracked VC air plasma sprayed APS TBC coatings are shown in Figure 1.

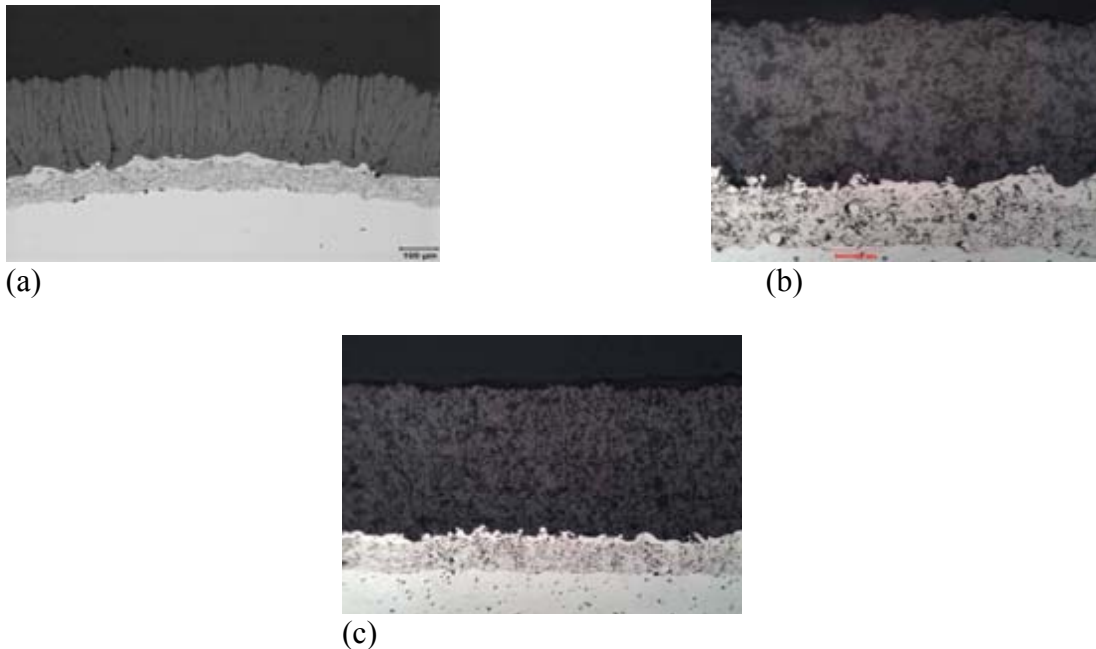


Fig.1 (a) EB-PVD and (b) standard APS and (c) vertically cracked VC APS coated TBC specimens microstructural images.

### 3.2 Thermo-physical Properties Characterization

For thermal property measurements, the TBC top coats were separated from the IN738 substrates using hydrochloric acid solution; then all the TBC samples were sputtering coated with a thin layer of platinum (< 1 micron), and then sprayed with high temperature grade graphite to eliminate any reflectivity provided by the Pt coating. The thermal properties of the coatings were measured on free-standing samples using a laser flash

system (FL5000) manufactured by ANTER Co according to the ASME E1461- 01. The Laser Flash method has been described extensively in the literature [14].

The characterization of the APS and EBPVD thermal barrier coatings was done by the study of density, thermal diffusivity, thermal conductivity, porosity, and microstructural analysis. The key step in density measurement is to find the volume of the sample. The density is first estimated via weight/volume. The thickness was measured using a micrometer (Mitutoyo, Model No. 2930832), range 0-1 in, graduations 0.0001 in. It is crucial to have the accurate thickness measurement as the overall thickness of the sample is two orders of magnitude smaller than the sample diameter. Thus, the thickness was also determined by scanning electron microscope (SEM). A weighing scale (Scientech ZSA 210) was used with a mass range 0.01g – 210 g, graduations of 0.0001 g.

During the Thermo-physical Properties Measurement, an instant pulse of laser power is applied to the front surface of the sample; this energy will be absorbed first and then conducted through the sample to the rear surface; and this produces an increase in the rear surface temperature of the sample. An infrared detector is used to record the temperature rise on the rear surface as a function of time. The analysis software uses “half time” to reach the maximum temperature to calculate the thermal diffusivity ( $\alpha$ ) using the following equation [14],

$$(\alpha) = 1388 .0 L^2 / t_{1/2}$$

where L is the thickness of the sample (cm) and  $t_{1/2}$  is the half time (s) to reach the maximum temperature rise. The thermal diffusivity values using this equipment have an accuracy of  $\pm 5\%$  and a reproducibility of  $\pm 3\%$  based on the manufacturer information.

Using FL5000, the specific heat ( $C_p$ ) of the samples was measured using an alumina reference sample. Both reference sample and the testing samples were coated using a thin layer of sputtered nickel and a spray of graphite coating, thus they have identical surface finishes. The reference method is based on the fact that the energy received by the TBCs samples and the reference sample would be the same under identical laser power. This can be expressed by the following equation,

$$(m \times C_p(T) \times \Delta T)_{ref} = (m \times C_p(T) \times \Delta T)_i$$

where  $m$  is the mass (kg),  $C_p$  is the specific heat (J/kg-K),  $\Delta T$  is the temperature rise of the sample under the laser power. For linear sensor, the detector signal (Volts) is proportional to the temperature change. For above equation,  $ref$  are the values for the reference material, and  $i$  are the values for the TBCs samples. The specific heat values calculated using laser flash system (FL5000), have an accuracy of  $\pm 6\%$  and a reproducibility of  $\pm 4\%$ , based on the manufacturer.

The thermal conductivity ( $k$ ) is calculated using the following equation,

$$k(T) = \alpha(T) \times C_p(T) \times \rho$$

where  $k$  is the thermal conductivity (W/m-K),  $\alpha(T)$  is the thermal diffusivity ( $\text{m}^2/\text{s}$ ),  $C_p$  is specific heat (J/kg-K), and  $\rho$  is the density ( $\text{kg}/\text{m}^3$ ).

The porosity measurements were carried out using POREMASTER 33 system manufactured by Quantachrome Instruments to determine porosity, pore size distribution, and pore number fraction. This method involves the intrusion of a non-wetting fluid (mercury) into the sample void by increasing the pressure of the fluid up to 33,000 psi. The equipment used is capable of measuring pore diameter down to  $0.0070 \mu\text{m}$ . The total porosity is calculated by measuring the total volume of mercury intruded into the sample and the bulk volume of the sample using the following equation [15],

$$\text{Porosity (\%)} = \frac{V_t}{V_b} \times 100$$

where  $V_t$  is the total volume of mercury intruded and  $V_b$  is the bulk volume of the sample.

Porosity tests were carried out of selected test samples for characterizations in different processing conditions of standard and VC and EB-PVD test samples. Samples were also characterized before and after thermocycling for comparison, two samples of each designation were used.

### 3.3 Thermal Oxidation and Cycling Studies

In the present study, TBC systems were investigated using NiCoCrAlYHf bond coats with YSZ TBC top coatings of  $300 \mu\text{m}$  and  $600 \mu\text{m}$  for both standard and VC APS TBC and  $300 \mu\text{m}$  thick EB-PVD YSZ top coatings to determine the effect of coating thickness and tailored microstructures in dry and wet thermal cyclic oxidation studies at elevated temperatures. The wet and dry thermal oxidation cycling studies were carried out at the Applied Research Laboratory, the Pennsylvania State University at  $1125^\circ\text{C}$  with a 1 hour cycle time in which the samples were held at temperature ( $1125^\circ\text{C}$ ) for 55 minutes followed by forced air cooling to room temperature. The thermal cycling tests for wet oxidation used the same 1 hr cycle but incorporated saturated water vapor to investigate oxidation behavior in moist environments.

The spalling resistance testing was carried out in a CM 1700 bottom loaded furnace using a 6 hour thermal cycle with ramping from  $25^\circ\text{C}$  to  $1200^\circ\text{C}$  in 30 minutes, soaked at  $1200^\circ\text{C}$  mode for 300 minutes, followed by cooling down from  $1200^\circ\text{C}$  to  $25^\circ\text{C}$  in 30 minutes. The YSZ coated superalloy materials with selective processed microstructures and thickness were evaluated for their spalling and delamination behavior. The behavior of coated materials related to processing and microstructure was investigated and modeled for their performance.

### 3.4 Hot Corrosion Type I and Type II Testing in Sulfur Environment

Industrial gas turbines are being designed to operate with a variety of fuels such as natural gas, syngas and fuels derived from gasified coal. One of the largest impurities in low grade coal is sulfur. Syngas produced using coal containing high amounts of sulfur results in increased hot corrosion of turbine components. Therefore, in order to evaluate the effects of syngas on the proposed materials, hot corrosion tests were performed on selected TBC samples. In order to evaluate the effects of syngas on the proposed materials, hot corrosion tests were carried out on both APS and EB-PVD YSZ coatings.

The TBC specimens for the study of resistance to hot corrosion Type I (900°C) and Type II (705°C) were processed using IN 738 substrate EDM machined pin specimens (3/16 inch diameter x 3 inch long), and as well as disc specimens, tumbled, and prepared with special bond coats containing Hf with chemical composition (wt.%) Ni-22Co-17Cr-12.5Al-0.25Hf- 0.4Si-0.6Y bond coats of about 125 µm and top coats of about 7.65 % yttria stabilized zirconia YSZ. In these hot corrosion tests, the top coat thickness was 300 µm and 600 µm YSZ for the standard and vertically cracked APS test pin specimens and 300 µm YSZ for EB-PVD coated specimens. In addition, the APS multi-sectioned specimens of TBC specimens processed with the bottom layer of top coats of about 150 µm of STD YSZ dense bottom layer with top layer of YSZ and composition variations of YSZ with 15%, 30% and 50% Al<sub>2</sub>O<sub>3</sub> content of about 150µm top layer were analyzed in comparison with standard and vertically cracked APS coated specimens and of the EBPVD multi-layered specimens. These specimens were evaluated for hot corrosion effects under Type I and Type II test conditions.

Testing under Type I and Type II hot corrosion conditions was carried out for durations from 20 to 100 hrs. The apparatus used for this testing was the Dean Rig test equipment at Applied Research Laboratory, the Pennsylvania State University, consisting of a multi-temperature zone furnace, alumina tube, molten sodium sulfate salt, and an O<sub>2</sub>-O.1%SO<sub>2</sub> gas mixture. At one end of the furnace, the O<sub>2</sub>- O.1%SO<sub>2</sub> carrier gas mixture is passed through a platinized honeycomb catalyst upstream from the crucible containing the sodium sulfate (contained in an alumina crucible) maintained at approximately 900oC (temperature above the sodium sulfate melting temperature of 884oC). The salt sprayed test specimens are then positioned in an alumina crucible (705oC) downstream from the molten sodium sulfate. The difference in temperature along the various zones of the furnace allows the vaporized sodium sulfate salt to condense onto the surface of the test specimens held at the lower temperature 705oC (Type II hot corrosion). Sodium sulfate salt is added to an alumina boat at the start of the experiment in order to maintain the equilibrium amount of SO<sub>3</sub> which stabilizes the activity of the sodium sulfate allowing an accelerated corrosion method of the test specimens. The salt sprayed specimens are then placed in an alumina tray contained in the lower temperature zone (705oC) of the Dean rig for evaluation under Type II hot corrosion conditions. Uncoated base alloy and YSZ coated standard and vertically cracked APS test specimens (300 µm and 600 µm thick), and 300 µm for EB-PVD coated specimens are being investigated for Type I and Type II hot corrosion conditions. The samples are tested for durations of a total of 100 hours in five 20-hour hot corrosion cycle increments.

Type II hot corrosion (low-temperature corrosion) generally occurs over the temperature range of 600-850 °C. Normally, Cr-rich and Al-rich alloys form a thin protective oxide ( $\text{Cr}_2\text{O}_3$  and  $\text{Al}_2\text{O}_3$ ) when exposed to oxygen-rich environments at elevated temperatures. Type II corrosion occurs when transition metals, such as nickel and cobalt from the uncoated base alloy, react with sulfur to form stable sulphates. These sulphates then react with alkali metal sulphates and form low melting point compounds that inhibit or restrict the growth of the protective passive oxide layer. Ni-Cr-Al-based metallic coatings have shown excellent resistance to Type II corrosion. In contrast, Type I hot corrosion starts when sulphatic deposits, such as  $\text{Na}_2\text{SO}_4$ , deposit on the protective oxide scale surface. Sulfur then diffuses across the protect oxide scale and forms a sulphide (most common is chromium sulfide) which are molten in the temperature range of 750°C to 950°C. In addition, other oxides such as nickel and cobalt sulfides can result in catastrophic degradation of GT components as the molten sulfides dissolve the protective oxide layer or prevent it from forming, and exposes the underlying superalloy. The Pt-modified nickel-aluminides and MCrAlX (>25%Cr and 6%Al) materials have shown the greatest resistance to Type I hot corrosion.

Thermally Grown Oxide (TGO) formed between the interface of the bond coat and the topcoat during the ceramic deposition is known to play a significant role in the hot corrosion and failure mechanisms. TGO generally consists of aluminum oxide. For NiCoCrAlY bond coats minor amount of spinels (Ni, Co)(Al,Cr) $_2\text{O}_4$  and occasionally NiO are also found particularly in the region closer to the bond coat [16-18]. The characteristics of the hot corrosion under Type I and Type II conditions have been of interest for applications of thermal barrier coatings in high temperature and gas turbine components [19-20]. In our work effects of hot corrosion of Type I and Type II have been investigated.

### 3.5 High Temperature Oxidation and Interfacial Growth Kinetics Studies

An experimental study of the high-temperature isothermal oxidation behavior and microstructural evolution in two variations of air plasma sprayed ceramic thermal barrier coatings (TBCs) was carried out. Two types of TBC specimens were produced for testing. These include a standard and vertically cracked APS. High temperature oxidation was carried out at 900, 1000, 1100 and 1200°C. The experiments were performed in air under isothermal conditions. At each temperature, the specimens were exposed for 25, 50, 75 and 100 h. The corresponding microstructures and microchemistries of the TBC layers were examined using scanning electron microscopy and energy dispersive X-ray spectroscopy. Changes in the dimensions of the thermally grown oxide layer were determined as functions of time and temperature. The evolution of bond coat microstructures/interdiffusion zones and thermally grown oxide layers were compared in the TBC specimens with standard and vertically cracked microstructures.

The test samples were prepared by APS with bond coats on a selected superalloy inconel (IN) 738 disks. The substrate samples were 12.5mm (0.5 in.) in diameter and 3.125mm (0.125 in.) in thickness. The bond coating composition used for the preparation of YSZ APS samples was a standard powder of nominal composition Ni-22Co-17Cr-12.5Al-



0.25Hf–0.4Si–0.6Y (% by weight). After bond coating was applied, the specimens were sprayed to produce the APS YSZ standard (STD-TBC) and vertically cracked (VC-TBC) samples. The bond coat and top coats were processed using APS process under selected spray conditions and precise gun-to-part motion for repeatability and control of the process. These plasma sprayed disc-shaped TBC specimens with STD and VC microstructures were heated isothermally and oxidized in air at 900, 1000, 1100 and 1200°C for durations of 25, 50, 75 and 100 h. For statistical reasons, three specimens were tested at each condition to check for variability in structure, composition and oxidation behavior. After heating, the samples were sectioned in half with a slow speed diamond saw. They were then mounted in conductive resin and ground with emery paper, prior to a final polish with 3M diamond hand pad.

After polishing, the specimen surfaces were coated with 5µm of carbon in an ion beam sputtering machine. The microstructures of the heat treated specimens were examined in a Phillips Model Q200 scanning electron microscope (SEM) and a FEI Model XL30 SEM. Semi-quantitative measurements of the microchemistries of the TBC layers were also obtained using energy dispersive X-ray spectroscopy (EDS) mapping during scanning electron microscopy in a Phillips Model Q200 SEM. These observations were used to provide insights into the effects of isothermal exposure on microstructure and microchemistry. The substrate microstructure was also investigated using a combination of electron back scatter diffraction (EBSD) and EDS maps of the specimen surfaces. The spatial resolution of the EBSD technique is about 100nm which enabled elucidation of the matrix and TBC composition and structure.

High temperature exposures were used to elucidate the microstructure changes in STD and VC processed APS structures. Changes in the dimensions of the TGO layer were also determined as functions of time and temperature. These were used to determine the kinetics of TGO growth. [21].

## **4. RESULTS AND DISCUSSION**

### **4.1 Thermo-physical Properties Characterization Results**

Tests of thermo-physical properties of the processed YSZ TBC samples have been carried out for determination of thermo-physical properties including porosity measurements and thermal conductivity at elevated temperatures up to 1300°C. Some of characteristic data of typical standard APS and VC microstructured specimens has been evaluated along with porosity measurements. [22-23]. As presented in [22] the plots of the processed VC samples that were characterized for thermal diffusivity and thermal conductivity up 1300°C are shown below. For samples of various processing conditions thermal conductivity and diffusivity data measured up to 800°C are presented in figures 3 and 4 below. Control of porosity and microstructure can have a significant impact on the thermal properties of the TBC materials.

Figures 2 and 3 depict experimental data of VC samples measured from 100 to 1300°C of thermal diffusivity and of thermal conductivity respectively. Apart from fourth data

point, the graph is well behaved and is monotonic decreasing. There is good agreement of the data in thermal diffusivity values from 0.003-0.007 cm<sup>2</sup>/s with values in the temperature range 200-800°C reported in the literature. This study has been able to achieve high temperature thermal properties measurement up to temperature of 1300°C.

This has been made possible by using a boron nitride spray coating on the surface of specimen to eliminate semi transparency effects of the YSZ that impedes the laser flash measurements. On the other hand, for lower temperatures below 800°C gold or platinum surface coating was appropriate as depicted in figures 2 and 3 below.

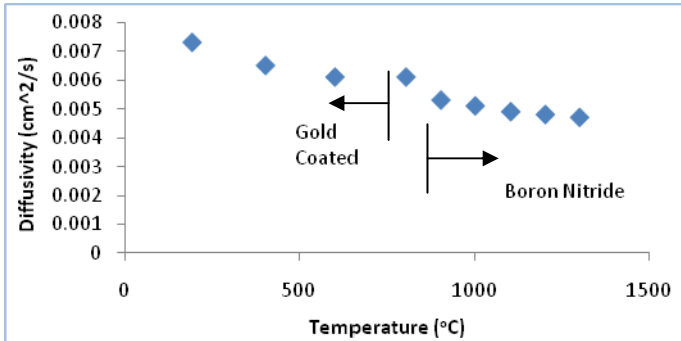


**Fig. 2 Thermal Diffusivity for APS VC 600 Sample**

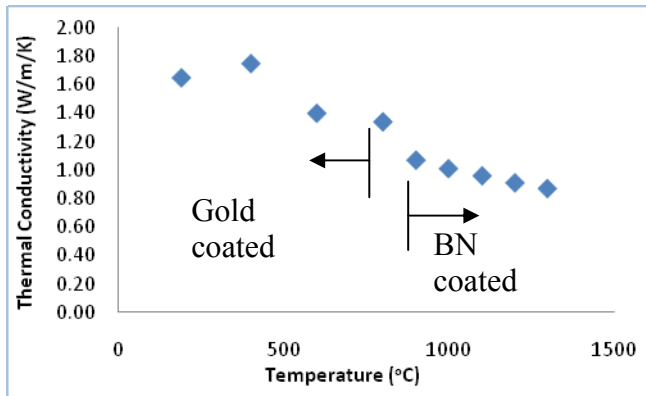


**Fig. 3 Thermal Conductivity for APS VC 600 Sample**

Thermal properties measurement data for different processing conditions and thickness of standalone top coats of STD and VC 300 and 600µm microstructures specimens is shown in Figures 4 and 5. The experimental results showed an increase in thermal diffusivity for the APS-VC samples compared with the APS-STD sample over the 400°C to 800°C temperature range tested. The APS-VC samples were found to have higher thermal diffusivity values than those of APS-STD. This is attributed to the vertical columnar microstructure in the APS-VC of the top coat layer. A thicker coating leads to a higher thermal diffusivity for both STD and VC.

The APS-VC samples have higher thermal conductivity than APS-STD samples. The columnar structure of the vertically cracked sample will facilitate the heat conduction within the sample. Thicker coatings have higher thermal conductivity and lower porosity due to the longer processing time (higher temperature) during plasma spray. The thermal conductivity for the APS samples has been reported to be in the range from 1.0 to 1.4 W/m-K by other researchers in the literature. Normally a higher value is expected for samples that have gone through a high temperature sintering and densification process. For the samples tested [23], the APS-STD300 samples are found to have the lowest thermal conductivity value compared with APS-STD600 and APS-VC300, and APS-VC600. This is believed to follow phonon-phonon scattering theory. The APS-VC samples have microstructure in between the perfect laminar structure (APS-STD) and the perfect columnar structure (EBPVD), thus the thermal conductivity values of APS-VC are expected to be larger than those of APS-STD samples and smaller than those of EBPVD samples.

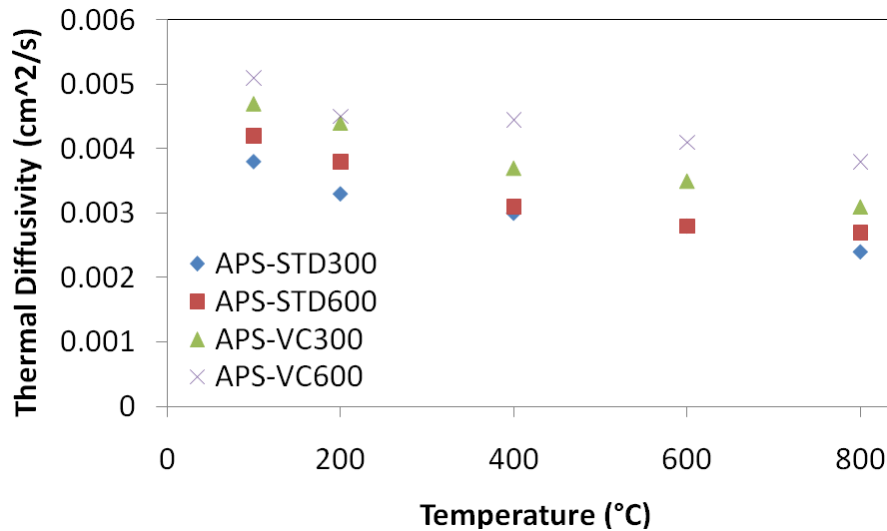


**Figure 4 Thermal Diffusivity for APS Samples with Standard and Vertically Cracked Microstructure**

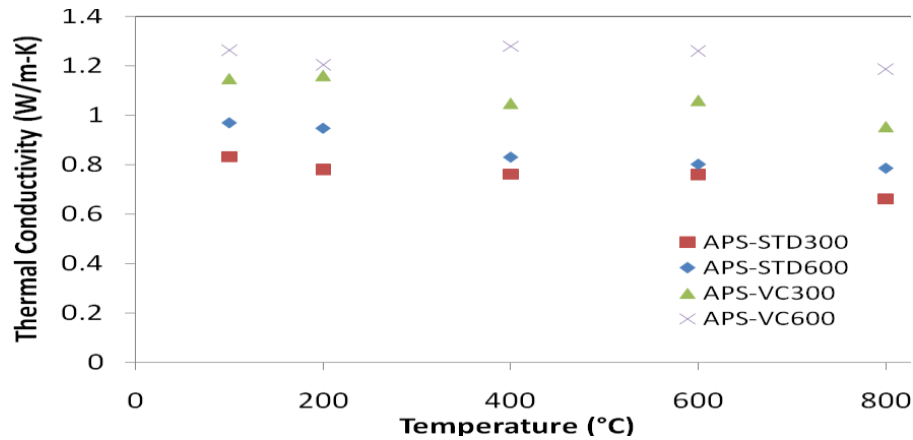


**Figure 5 Thermal Conductivity for APS Samples with Standard and Vertically Cracked Microstructure**

Porosity of the plasma sprayed standard (STD) APS and vertically cracked (VC) APS thermal barrier coatings for two different thicknesses, 300 and 600  $\mu\text{m}$  respectively and of EB-PVD of 300  $\mu\text{m}$  thickness TBCs have been analyzed to compare the effects of the microstructure and porosity on the behavior of the TBCs at elevated temperatures. Representative results of porosity as measured are shown below in Table 1 comparing different processed TBC samples of varying thickness as well as processing conditions. [23]. For EBPVD specimens, NT refers to not tumbled specimen condition and T refers to tumbled condition of the disk samples prior to EBPVD coatings. All APS samples had been tumbled prior to processing.

**Table 1. Porosity Results for APS and EBPVD Samples**

SAMPLE ID	Porosity (%)
APS-STD300	17.4
APS-STD600	7.8
APS-VC300	14.6
APS-VC600	5.2
EBPVD-T300	13.3
EBPVD-NT300	12.1

As it is shown in the table above, the high values of porosity are found for the APS-STD samples; the values are 17% for samples of 300 $\mu\text{m}$  thick and 7.8% for 600  $\mu\text{m}$  thick samples. For the thicker coating the processing time is longer than that of thinner coatings, thus the thicker coating is prone to exhibit sintering due to the high temperature in the atmospheric plasma spray process. In comparison, the APS-VC samples have lower porosity than those of APS-STD samples; the values are 14.6 % for samples of 300  $\mu\text{m}$  thick and 5.2 % for samples 600  $\mu\text{m}$  thick samples. To prepare the vertical cracked samples, the substrate is preheated to a very high temperature. It produces a grain growth in columnar structure within the splats. During this heating process the APS ceramic coating experiences sintering, and then the samples become denser if the processing time is longer, which is the case for the thicker coatings. This is also confirmed by the density values estimated by weight/volume and Archimedes Method. A dense coating with high density values will have lower porosity and vice versa. On the other hand, for

the EBPVD samples the porosity values are lower than APS-STD300, which are about 13 % for both tumbled and not - tumbled samples. In addition, the porosity is lower compared to APS-VC300, wherein, it seems that the columnar structure made by electron beam physical vapor deposition leads to a lower porosity coatings for the same thickness.

The pore size distribution by volume and by fraction for APS-STD and APS-VC samples are presented in Fig. 6 and Fig. 7, respectively. The thicker samples have fine pores as the peak in the pore size distribution function graph is shifted to smaller values if the APS-STD600 is compared with APS-STD300. Also, the same phenomenon is observed for APS-VC.

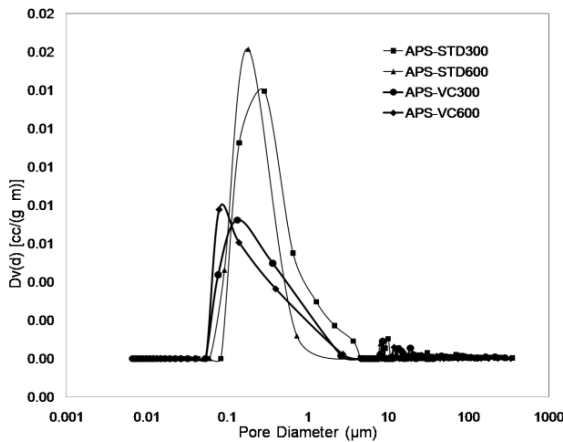


**Figure 6. Pore Size Distribution Function of APS-STD and APS-VC Coatings**

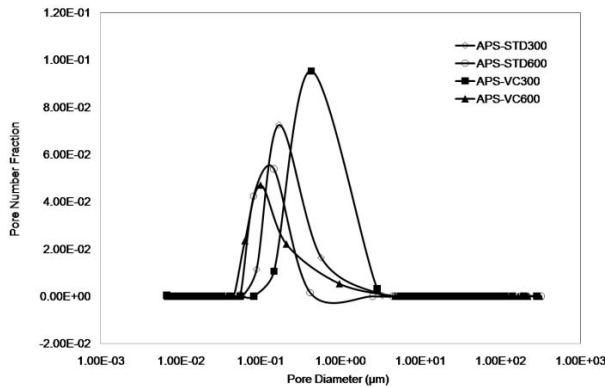


**Figure 7. Pore Number Fraction of APS-STD and APS-VC coatings**

The samples made with 300 μm thickness have larger pore sizes compared to samples with thickness of 600 μm for APS-STD and APS-VC, Fig. 7. This is evidence that thicker samples experienced sintering during the atmospheric plasma spray process. Also it is noticeable the difference between the pores sizes for APS-STD and for APS-VC.

SEM images of free-standing coatings cross section and top morphology of all samples were taken. The SEM images of APS-STD and APS-VC are presented in Figures 8 -10. The fractured cross-section of APS-STD 300 coatings are shown in Figure 8(a). As shown, the microstructure

is characterized by a lamellar structure; APS-STD 300 coating showed layers or splats along the thickness of the coating. Interlamellar cracks (IC), are evident for both thicknesses of 300 and 600 microns samples. Defects such as IC will provide significantly reduction of thermal conductivity. Other features, such as close pores (CP), globular pores (GP), and interlamellar cracks (IC), can also be observed in the atmospheric plasma spray coating. These characteristics should be carefully controlled to provide better properties of the coating. Defects such as interlamellar pores will provide significantly reduction of thermal conductivity, but it will cause premature failure due to poor adhesion between splats within the coatings.

As expected, thicker coating APS-STD 600 has dense structure, these coatings still have lamellae structure but the adhesion between splats is better than the APS-STD 300 coating. As it is shown in Figure 8, a dense structure is also observed for a thicker coating. This defect appears because longer processing time is needed for creating the thick coating. For the APS-STD 600, there are still some interlamellar cracks (IC) but the lamellae structure is more cohesive. Also, the thickness of the splats is reduced from 10  $\mu\text{m}$  for APS-STD 300 to 5 $\mu\text{m}$  for APS-STD 600 coatings, which is indicative of the sintering of the coating occurring during coating deposition and thermal cycling.

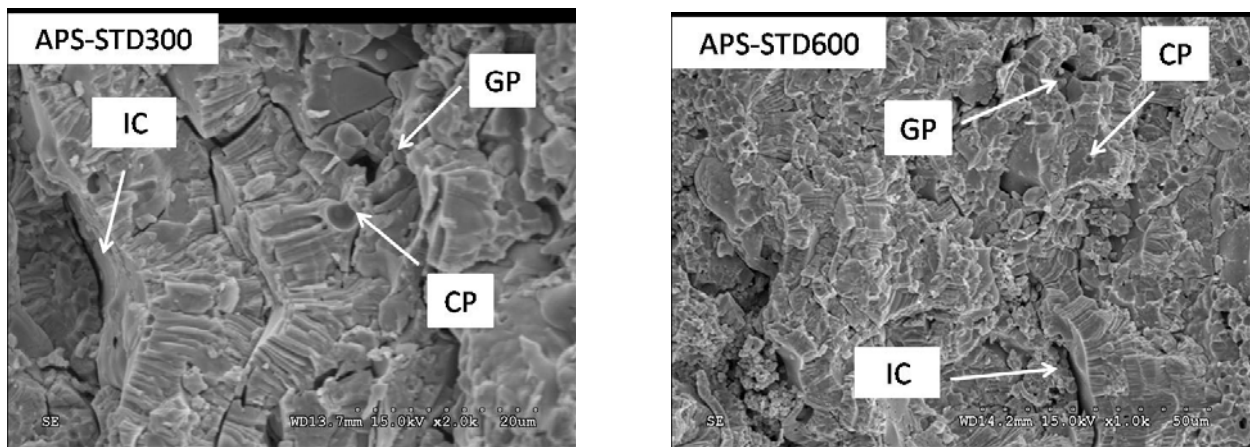


Figure 8 (a) SEM Micrograph of APS-STD300 and (b) SEM Micrograph of APS-STD600

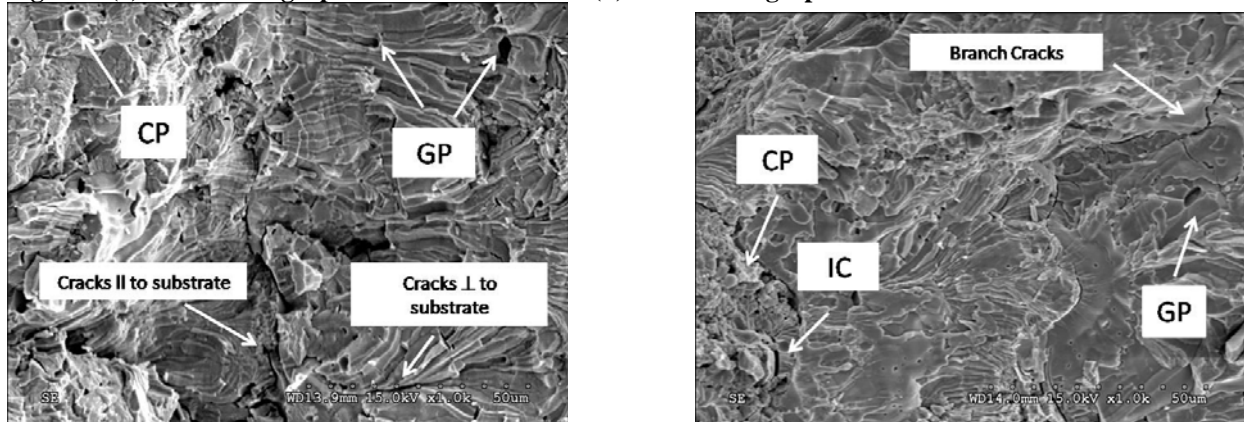
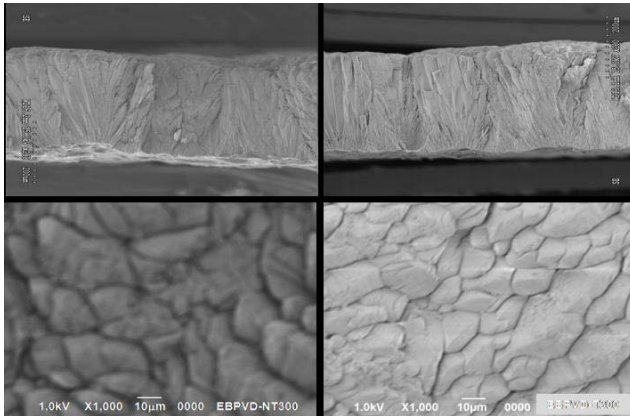


Figure 9 (a) SEM Micrograph of APS-VC300 and (b) SEM Micrograph of APS-VC600

For the APS-VC samples, the grain structures are aligned in the vertical direction with respect to the cross-section area and the coating has multiple cracks in the same direction, as it is shown in Figure 9. This microstructure enhanced the heat transfer along the vertical direction and strongly influenced the increase of thermal conductivity observed for those samples. The thermo-physical property changes are directly linked to the samples microstructures demonstrated by the measured thermal properties and confirmed by SEM images.

In addition, for thicker coatings, APS-VC 600, branch cracks as well as vertical cracks are observed within the thickness of the coating. The formation of branch cracks or vertical cracks is usually due to the mismatch between the substrate and the coating. The cracks are initiated in the surface of the coating and propagated within the thickness. As it is shown in the SEM micrographs, the APS-VC 600 has a denser structure compared to APS-VC 300.

The SEM images for EBPVD cross section and top morphology before thermal cycling are shown in Figure 10. As shown in the images and also reported in the literature, the top coat manufactured by electron beam physical vapor deposition is characterized by a columnar structure. The columns are made out of almost single columns starting from the substrate with very small size (around 2-3  $\mu\text{m}$  in diameter) and grow through the thickness of the coating up to thicker tip in the surface of the coating (about 10 – 20  $\mu\text{m}$ ).



**Figure 10 SEM micrographs of two different EBPVD coatings before heat treatment. Top: Cross section images of the free-standing top layer. Bottom: morphology of top surface of the coatings.**

#### 4.2 Thermal Oxidation and Cycling Characterization Results

For studying the effects of different microstructured regimes and to predict the performance of TBC materials wet and dry thermal oxidation cycling experiments were carried out at 1125°C. The results of the wet and dry thermal cyclic furnace testing at 1125 °C are reported in Figure 11 and 12. As shown in Figure 11 the average number of cycles to failure for the standard plasma spray APS STD, vertically cracked plasma spray APS-VC, and EB-PVD tumbled EBPVD-T TBC coatings was 232, 297 and 417 respectively for the wet thermal cyclic testing. There was a slight improvement in the average number of cycles to failure for the vertically cracked samples as compared to the standard plasma spray APS coatings. In Figure 12 the average number of cycles to failure for the standard plasma spray APS-STD, vertically cracked plasma spray APS-VC, EB-PVD tumbled EBPVD-T and EB-PVD non-tumbled EBPVD-NT TBC coatings was 463, 360, 1012 and 642 respectively for the dry thermal cyclic testing. Wet and dry cyclic furnace

testing results are presented of the average cycles to failure in Figure 11 and 12 below with five samples used for each rest condition.

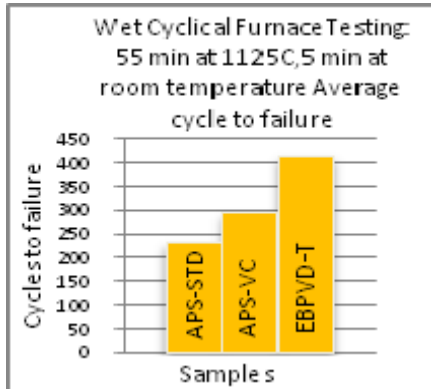


Figure 11. Wet Cyclical Furnace Test Results.

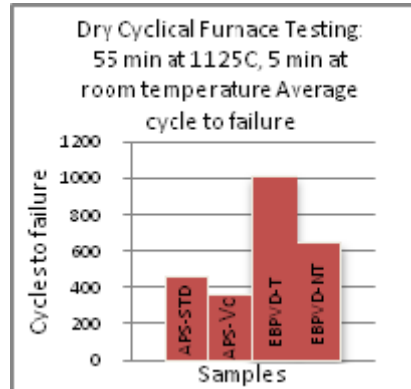


Figure 12. Dry Cyclical Furnace Test Results.

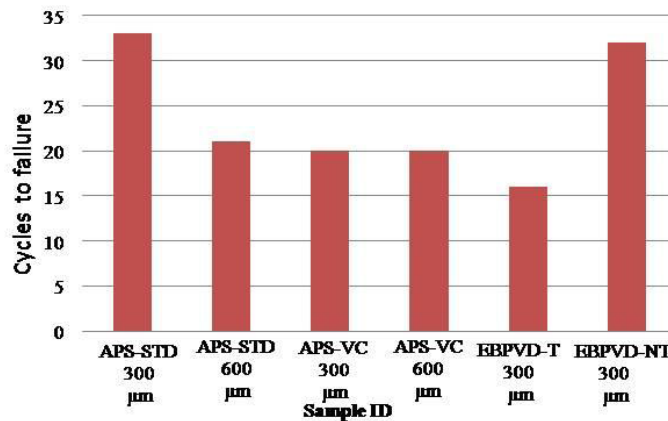


Figure 13 Thermal Cycling Results for APS and EBPVD

#### 4.3 Hot Corrosion Type I and Type II Testing Results

The results of the hot corrosion testing of the uncoated and the coated APS and EBPVD TBC samples were analyzed for periods up to 100 hrs under Type I (900°C) and Type II (705°C) test conditions. The several samples tested indicate the best resistance to hot corrosion in case of the EB-PVD and columnar structures. However, specimens with higher coating thickness in case of the APS specimens appear to have higher hot corrosion resistance for Type I and Type II test conditions. Other factors could also be impacting on the hot corrosion effects. Rough surface finish will tend to facilitate better mechanical adhesion and processing of columnar structure appears to help in achieving more strain tolerant microstructural top ceramic coatings of the TBC specimens.

The processed multi-layer APS and EBPVD samples were also evaluated for hot corrosion effects as carried out with two configurations of 70% YSZ / 30% Alumina ratio and of 85% YSZ / 15% Alumina ratio. After completion of 100 hours of Type II testing, it appears that all of the samples tested show a pattern of increased corrosion with increasing exposure to the hot corrosion environment (i.e., each 20 hour increment). The EB-PVD samples with an expected 70% YSZ / 30% Alumina ratio appeared to have performed the best, even though salt/corrosion



penetration between the TBC columns was observed, but with little damage to the bond coat. There was difficulty in processing of EBPVD multi-layer specimens and the desired coating thickness for the EB-PVD coatings and composite layers were thinner than expected.

In our evaluations of Type I hot corrosion testing of the processed multi-layer APS and EBPVD samples the results of the STD APS samples with about 70 %YSZ/30 % Alumina appeared to have performed the best though under these severe conditions the salt/corrosion penetration at the TBC /bond interface was observed. As noted previously, EBPVD specimens of 85 %YSZ/15%Alumina and 70 %YSZ/30% Alumina coatings were difficult to be processed and the composite layers in these were thinner than expected. These EBPVD tested samples showed salt/corrosion penetration between TBC columns.

#### 4.4 High Temperature Interfacial Growth Kinetics and TGO studies

The results of an experimental study of the high-temperature isothermal oxidation behavior and microstructural evolution in two variations of air plasma sprayed ceramic thermal barrier coatings (TBCs) as described in section 3.5 of this report are discussed in this section.

Plots of the TGO thickness ( $\mu\text{m}$ ) versus the square root of time,  $t(\text{s})$ , are presented in Figures 14a for isothermal oxidation at 900, 1000 and 1100°C for STD TBC and VC TBC respectively. The linear plots are a clear indication that the interfacial growth kinetics is parabolic as reported by others in the literature. Hence, the oxide thicknesses should reach different plateau levels, unless the underlying interdiffusion mechanisms change with increasing duration of isothermal exposure. Furthermore, in an effort to identify the chemical species that control the growth of the TGO layers, the reaction rates,  $k$ , were obtained from the rate axis intercepts of the lines in Figures 14a. The measured values of  $k$  are presented in Figure 14b, for the STD and VC microstructures respectively. The results are plotted as Arrhenius functions of the inverse of the absolute temperature, for temperatures of 900, 1000 and 1100°C. Within this temperature regime, the activation energies were determined to be 437 kJ/mol for STD TBC and 484 kJ/mol for the VC TBC. These correspond to the activation energy for the diffusion of  $\text{O}_2$  in  $\text{Al}_2\text{O}_3$  suggesting that the growth kinetics of the TGO is kinetically limited by the diffusion of  $\text{O}_2$  and  $\text{Al}_2\text{O}_3$ . As shown in Figure 14b, the activation energy obtained by Madhwal et al. [24] (446 kJ/mol  $\pm 60$  kJ/mol) compares very favorably with our results for the VC TBC (484 kJ/mol) although a different temperature range was used in that study.

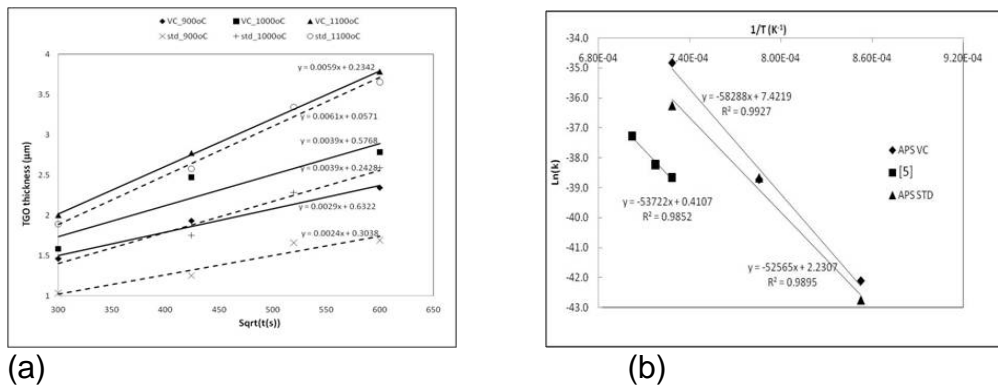


**Figure 14 (a) Oxide Thickness (mm) vs Square root of Time(s) for APS STD TBC and APS VC TBC**  
**(b) A Plot of Natural Logarithm of Rate Constant against Inverse of absolute Temperature for APS VC TBC and APS STD TBC**

#### 4.5 In-service Performance Thermo-Elastic Computational Modeling for TBC Failure Analysis

TBCs subjected to thermal cycling and mechanical loading resulting in tension or bending may have different failure modes such as spallation, delamination, debonding, etc [25]. Failure has been shown to be predominately initiated at the bond coat/TBC interface region where the interface may have an imperfection, undulating/wrinkle, rumpling strain or can arise as a result of damage by foreign object. For APS TBC coated systems, investigators have shown that failure initiates either in the TGO [26,27] or typically at a close distance to the TBC/TGO interface [27-29]. These initiation cracks coalesce and propagate within the TBC parallel to the interface, causing spallation as a result of compressive stress on the TBC during cycling. On the other hand, EB-PVD coating fail by cracking along the TGO-bond coat-face [29, 31-33]. This difference in failure mechanism is primarily attributed to the difference in the microstructure of the TBC as the EB-PVD is more strain compliant. APS coatings are porous due to processing with a relatively non-uniform distribution of micro-cracks that weaken its fracture toughness ( $\approx 0.5 \text{ MPa}\sqrt{\text{m}}$ ) [34]. EB-PVD coatings consist of loosely interconnected columnar grains, usually oriented normal to the coating/substrate interface. As a result, the EB-PVD coating is reported to be more strain tolerant in direction perpendicular to the columns (in-plane coating directions) and thus more resistant to crack growth compared with the APS coatings. Another significant difference between the two systems is the morphology of the bond coat/TBC interface: in APS systems adhesion is mechanical, ensured by means of a rough interface that promotes layer interlocking, while in EB-PVD coatings interfacial adhesion is chemical and interfaces are smooth.

The goal of this study was to investigate the thermo-elastic behavior that leads to TBC failure by considering the potential mechanisms of loading and thermal cycling to understand and model the critical parameters for TBC failure. The approach used was (i) to develop a model that predicts thermal gradients in-situ of TBC overlaid on typical gas turbine blade exposed to high thermal loads during in-service application, (ii) then develop a preliminary model for the prediction of creep and crack growth in thermally sprayed NiCoCrAlY thermal barrier coatings subjected to isothermal and cyclic oxidation conditions, and (iii) finally, determine delamination size (crack growth), TGO thickness and modulus to be used in the classical plate theory for predicting buckling as a failure mode.

(i) Prediction of thermal gradients in-situ of TBC overlaid on typical gas turbine blade exposed to high thermal loads during in-service application

This study focuses on the estimation of temperature distribution in the turbine metal substrate (IN738) and coating materials (EBPVD TBC and APS TBC) subjected to isothermal conditions (1573 K) around the turbine blade. The heat conduction in the turbine blade and TBC systems necessary for the evaluation of substrate thermal loads are assessed. The steady state 2D heat diffusion in the turbine blade is modeled using ANSYS FLUENT computational fluid dynamics (CFD) commercial software. Heat transfer by radiation is fully accounted for by solving the radiative transport equation (RTE) using the discrete ordinate method.

The results as we reported in [35] show that APS TBCs are better heat flux suppressors than EBPVD TBCs due to differences in the morphology of the porosity present within the TBC

layer. Increased temperature drops across the TBC leads to temperature reductions at the TGO/bond coat interface which slows the rate of the thermally induced failure mechanisms such as CTE mismatch strain in the TGO layer, growth rate of TGO, and impurity diffusion within the bond coat.

Figure 15 shows the temperature variation across the TBC system in the Y-direction at a fixed X-location ( $X = 0.09\text{m}$ , mid-chord length) for the cases with APS TBC and EBPVD TBC. From the plot it is clear that the use of TBC causes the metal temperature to drop by about 100K justifying why most researchers consider the use of TBC coupled with effective cooling technique as heat suppressor for high temperature applications. The amount of temperature drop for the APS TBC is slightly greater than the drop for EBPVD TBC. This can be explained by the differences in the coating microstructure, porosity contents, pore morphologies and orientations. In APS layers, inter-splat pores result from the impingement of molten droplets onto a substrate. The pores align themselves parallel to the substrate surface and are accompanied by microcracks and fine grain boundaries. It is known that the thermal conductivity of TBCs decreases with increase in porosity. The pore volume fraction provides a high impedance of heat flow through the TBC thickness resulting in a TBC layer of low thermal conductivity. Conversely, EBPVD TBCs have columnar microstructure with elongated intercolumnar pores that become aligned perpendicular to the plane of coating as the thickness increases. The elongated intercolumnar pores increase the compliance of the coating in the plane of the substrate and leads to the improved spallation lifetimes of the TBC systems.

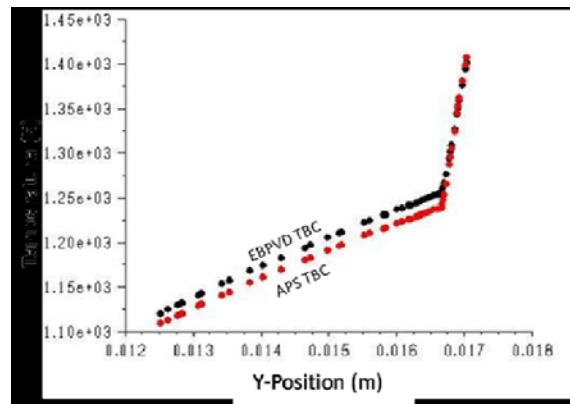


Figure 15 Temperature Distribution at  $X = 0.09\text{m}$  from the leading edge of the blade with TBC and radiation for EBPVD and APS TBCs

The temperature drop is of significance to turbine researchers since it determines the eventual temperature distribution of the metal substrate and cooling load requirements. Furthermore it is speculated that metal temperature drop of about 30 to 60 °C has the potential to increase hot gas path components' lives by a factor of 2.

The temperature contours in the metal substrate and the thermal barrier coating is given in Figure 16 for the case of APS TBC. There is high concentration of heat flux at the leading and trailing edges of the blade, which makes these areas the hot spots of the turbine blade. More effective cooling techniques such as film cooling, jet impingement or fins orthogonal to the coolant flow can be used to mitigate the excessive heat flux at the hot spots.

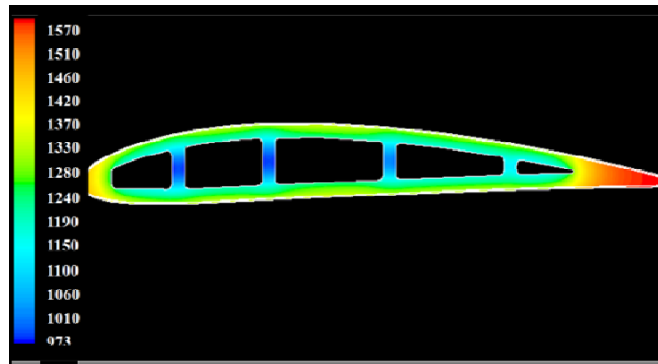


Figure 16 Temperature Distribution of Turbine Blade Subjected to Isothermal Conditions External to the Top Coat.

The plot shown in Figure 17 indicates the effects of radiation and TBC on temperature distribution in the metal substrate. In segment A of the plot, both TBC and radiation were applied to the simulation model. The temperature of a reference point in the substrate located at  $x = 0.09\text{m}$  and  $y = 0.0164\text{m}$ , which is one bond coat thickness below the bond coat-substrate interface, approached the steady state temperature, 1240K, after about 30 iterations. In segment B, TBC was used without radiation on the external top coat. The temperature distribution is underpredicted. The trends in the temperature distribution for segments C and D are similar to the trends in A and B. In fact the temperature of metal substrate without TBC with radiation is about 1340K (section D of Figure 17). The use of TBC dropped the metal substrate temperature to about 1240K (section A of Figure 17), a drop of about 100K. In general coatings provide a thermal barrier effect, in which a large temperature gradient takes place across the coating layer, substantially lowering the substrate temperature necessitating a decrease in cooling load which eventually saves operational/research dollars.

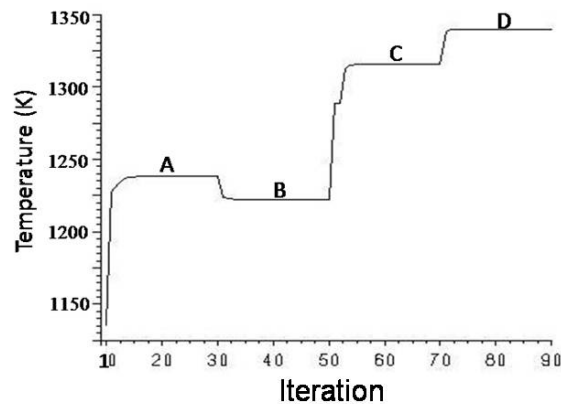


Figure 17 Area weighted Average Temperature History at point  $X = 0.09\text{m}$  and  $Y = 0.0164\text{m}$  for Various Simulation Models: A = TBC + Radiation; B = TBC - Radiation; C = - TBC - Radiation; D = -TBC + Radiation; “+” means with and “-” means without.

#### 4. KEY OUTCOMES

As part of this funded research three graduate students completed their Master's thesis at Southern University and one graduate student completed Ph.D. dissertation work on related thermal barrier coatings characterization and performance. In addition, two research associates received part of their funding for their work on this project.

Following research publications and conference proceedings papers also resulted during performance of this research period.

##### **Publications:**

1. Ravinder M. Diwan (PI), Patrick F. Mensah and Guoqiang Li, (Co-PIs) , Southern University, Baton Rouge, LA and Douglas Wolfe , Pennsylvania State University and Purush Sahoo, Materials Solutions International MSI Inc, Houston, Texas, "A study of Advanced Materials for Gas Turbine Coatings at Elevated Temperatures Using Selected Microstructures and Characteristic Environments for Syngas Combustion", Abstract, 2008 DOE UCR/HBCU OMI Conference, Pittsburgh, PA, June 10-11, 2008.
2. Monica B. Silva, S.M. Guo, Nalini Uppu, Ravinder Diwan, Patrick F. Mensah, "Thermal Property Measurements of YSZ-Al<sub>2</sub>O<sub>3</sub> Ceramic Composites", Proceedings of ASME Turbo Expo 2009: Power for Land, Sea and Air, June 8-12, 2009, GT 2009- 59496.
3. Monica B. Silva, S.M. Guo, Nalini Uppu, Ravinder Diwan, Patrick F. Mensah, "Porosity Effects on Thermo-physical Properties of Standard and Vertically Cracked Thermal Barrier Coating Samples", Proceedings of ASME Turbo Expo 2009: Power for Land, Sea and Air GT June 8-12, 2009, GT 2009- 59826.
4. Dr. Ravinder M. Diwan (PI), Dr. Patrick F. Mensah and Dr. Guoqiang Li, (Co-PIs) , Southern University, Baton Rouge, LA. "A study of Advanced Materials for Gas Turbine Coatings at Elevated Temperatures Using Selected Microstructures and Characteristic Environments for Syngas Combustion", Abstract, Presentation 2009 DOE UCR/HBCU OMI Conference, Morgantown, WV, June 9-10, 2009.
5. Ravinder M. Diwan, Patrick F. Mensah, Ogad Agu, and Douglas E. Wolfe, "Thermal Oxidation Cycling Studies of APS and EB-PVD Composite TBC Microstructured Coatings", ICCE/Nanoengineering Conference ICCE-17, Honolulu, Hawaii, July 26-31, 2009.
6. Stephen Akwaboa, Monica B. Silva, Patrick Mensah, Ravinder Diwan, Douglas E. Wolfe, and Shengmin Guo, "Comparison of Cyclic Oxidation Performance of APS and EBPVD Processed TBCs On IN 738 with a Bond Coat of NiCoCrAlY Powder with 0.25% Hf", Proceedings of the ASME 2009 International Mechanical Engineering Congress & Exposition, November 13-19, 2009, IMECE 2009-11901.
7. Winston Soboyejo, Patrick Mensah, and Ravinder Diwan, "Interfacial Kinetics of High Temperature Oxidation in YSZ Thermal Barrier Coatings with Bond Coatings of NiCoCrAlY

with 0.25% Hf”, Proceedings of the ASME 2009 International Mechanical Engineering Congress & Exposition, November 13-19, 2009, IMECE 2009-11556.

8. Ravinder M. Diwan, Patrick F. Mensah, and Douglas E. Wolfe, “High Temperature Oxidation and Hot Corrosion Studies of APS and EB-PVD Advanced Thermal Barrier Coatings”, Abstract, Presentation African Materials Research Conference, Abuja, Nigeria, 2009 A-MRS, December 14-18, 2009.

9. Dr. Ravinder M. Diwan (PI), Dr. Patrick F. Mensah and Dr. Guoqiang Li, (Co-PIs) , Southern University, Baton Rouge, LA.

“A study of Advanced Materials for Gas Turbine Coatings at Elevated Temperatures Using Selected Microstructures and Characteristic Environments for Syngas Combustion”, Abstract, Presentation 2010 DOE UCR/HBCU OMI Conference, Pittsburgh, PA, June 2-3, 2010.

10. Ogad Agu, Ravinder Diwan, Patrick F. Mensah, Monica B. Silva, and S.M. Guo, “Porosity and Thermal Cycling Behavior of Plasma Sprayed and EB-PVD Thermal Barrier Coatings”, Proceedings of ASME Turbo Expo 2010: Power for Land, Sea and Air GT June 14-18, 2010, GT 2010- 22433.

11. Stephen Akwaboa and Patrick F. Mensah, “Effects of Thermal Radiation on Air Plasma Spray (APS) Coated Gas Turbine Blade”, Proceedings of 14<sup>th</sup> International Heat Transfer Conference, IHTC 14, August 8-13, Washington DC, IHTC14-22961.

12. Monica B. Silva, S.M. Guo, Patrick F. Mensah, and Ravinder Diwan, “Thermal Conductivity Prediction for Thermal Barrier Coatings”, Proceedings of the ASME 2010 International Mechanical Engineering Congress & Exposition, November 12-18, 2010, Vancouver, British Columbia, Canada, IMECE 2010-38728.

13. Ravinder M. Diwan, Patrick F. Mensah, Naresh Polasa, and Douglas E. Wolfe, “Hot Corrosion and Thermal Oxidation of EB-PVD and APS Thermal Barrier Coatings”, ICCE/Nanoengineering Conference ICCE-18, Anchorage, Alaska, July 4-10, 2010.

14. W. O. Soboyejo, P. Mensah, R. Diwan, J. Crowe, S. Akwaboa, “High Temperature Oxidation interfacial Growth Kinetics in YSZ Thermal Barrier Coatings with Bond Coatings of NiCoCrAlY with 0.25% Hf”, Journal Article, Materials Science and Engineering A 528 (2011) 2223-2230.

## 5. CONCLUSIONS

- A NiCoCrAlY with 0.25% Hf bond coat formulation has been used on IN 738 superalloy substrate materials to process the standard and vertically cracked APS microstructured TBC specimens. These have provided comparative microstructured regimes that have been tested along with EB-PVD test specimen for effects of microstructure on the performance behavior of the TBC materials using YSZ topcoats and combinations of multi-layered TBCs including YSZ and variations of alumina.

- The APS-VC specimens have exhibited similar columnar structure as seen in EB-PVD processed specimens. The porosity effects and thermo-physical properties have been characterized in detail of the TBC samples up to 1300°C and the properties have been correlated with microstructural effects. The porosity measurements reveal that a thicker coating has lower porosity, for both APS-STD and APS-VC samples. Furthermore, the APS-VC samples were found to have lower porosity than those of APS-STD samples.
- EB-PVD specimens and APS-STD and APS-VC specimens have been tested for hot corrosion and wet and dry thermal cycling performance of selected TBC samples. The wet and dry thermal cycling results at 1125°C showed that there was a slight improvement in the average number of cycles to failure for the APS-VC samples as compared to the APS-STD coatings in case of wet thermal cycling and in dry thermal cycling the EB-PVD specimens behaved better.
- Thermal cycling behaviors of TBC samples heated up to 1200 °C were also investigated. In terms of the lifetime results, there is no conclusive evidence that APS-VC have a particular advantage over APS-STD at 1200 °C cycling behavior. It seems that APS-STD structure has a good strain tolerance under high working temperature of 1200 °C.
- Hot corrosion Type I and Type II tests have been carried out of the uncoated and the coated TBC samples for periods up to 100 hrs under Type I (900°C) and Type II (705°C) test conditions. The several samples tested indicate the best resistance to hot corrosion in case of the EB-PVD and columnar structures. However, specimens with higher coating thickness in case of the APS specimens appear to have higher hot corrosion resistance for Type I and Type II test conditions.
- Hot corrosion Type I and Type II tests were also conducted for the multi-layered TBC specimens with 70% YSZ / 30% Alumina ratio and of 85% YSZ / 15% Alumina ratio in top coats. After completion of 100 hours of Type II testing, the EB-PVD samples with an expected 70% YSZ / 30% Alumina ratio appeared to have performed the best, even though salt/corrosion penetration between the TBC columns was observed, but with little damage to the bond coat. In the Type I more severe hot corrosion of the processed multi-layered APS and EB-PVD samples the results of the APS-STD samples with about 70 %YSZ/30 % Alumina appeared to have performed the best. It should be noted that EB-PVD specimens of 85 %YSZ/15%Alumina and 70 %YSZ/30% Alumina coatings were difficult to be processed and the composite layers in these were thinner than expected.
- A thermal performance assessment model has been developed that can be used to predict temperature gradients in TBC systems. A kinetics model has also been developed based on experimental isothermal oxidation studies to predict the growth of TGO at elevated temperatures. These two models when coupled together will aid in investigating the thermo-elastic behavior that could lead to TBC failure due to growth stresses at TGO interfaces.

## 6. REFERENCES

- 1 D.M. Gray, Y. Lau, C.A. Johnson, M.P. Borom, W.A. Nelson, "Thermal barrier coatings having an improved columnar microstructure", United States Patent 5830586 (1998)
- 2 J. T. Demas-Marcin, K. D. J.T. Sheffler, M. Ortiz, "Thermal Barrier Coatings Life Prediction Model, Phase I," NASA CR-182239 (1989)
- 3 S. M. Meier, D. M. Nilsen, K. D. Sheffler, "Thermal Barrier Coating Life Prediction Model Development, Phase II," NASA CR-189111 (1991)
- 4 N.R. Shankar, C.C. Berndt, H. Herman, "Characterization of Mechanical Properties of Plasma-Sprayed Coatings," Advance in Materials Characterization, D.R. Rossington, R.A. Condrate, and R.L. Snyder, Ed. Plenum, (1983) pp. 473-489
- 5 H. Wang and W. Montasser, "Degradation of Bond Coat Strength under Thermal Cycling- Technical Note," Journal of Thermal Spray Technology, 2(1) (1993) pp. 31-34
- 6 A. K. Ray, N. Roy, A. Kar, A. K. Ray, S. C. Bose, G. Das, J. K. Sahu, D. K. Das, B. Venekataraman, S. V. Joshi, Material Science and Engineering A 505 (2009) pp. 96-104
- 7 D. Pan, M. W. Chen, P. K. Wright, K. J. Hemker, "Evolution of the diffusion aluminide bond coat for thermal barrier coatings during thermal cycling," Acta Materialia 51 (2003) pp. 2205-2217
- 8 A. Bartlett, R. J. Dal Maschio, "Failure mechanisms of a zirconia-8 wt% yttria thermal barrier coating," Journal of American Society 78 (4) (1995) pp. 1018
- 9 D. M. Nissley, "Thermal barrier coating life modeling in aircraft gas turbine engines ," Journal of Thermal Spray Technology 6 (1) (1997) pp. 91
- 10 G. M. Newaz, S. Q. Nusier, Z. A. Chaudhury, "Damage accumulation mechanisms in thermal barrier coatings," Journal of Engineering Materials and Technology, 120(2) (1998) pp. 149-153
- 11 E. Tzimas, H. Mullejans, S. D> Peteves, J. Bressers, W. Stamm, "Failure of Thermal Barrier Coating Systems under Cyclic Thermomechanical Loading," Acta Materialia 48 (2000) pp. 4699-4707
- 12 S. Bose, "High Temperature Coatings," Publisher: Butterworth-Heinemann, (2007)
- 13 D. Wolfe, J. Singh, R. Miller, J. Eldridge, D. Zhu, "Tailored microstructure of EB-PVD 8YSZ thermal Barrier Coatings with Low Thermal Conductivity and high thermal reflectivity for turbine applications," Surface & Coatings Technology, 190 (2005) pp. 132-149
- 14 Lin, B., Li, C., Su, C., Ban, H., Scripa, R. N. and Lehoczky, S. L., 2005, "Laser Flash Method for non-opaque materials," Proceedings of HT 2005, 1 (2005) pp. 777-785.



- 15 Quantachrome Instruments, POREMASTER Operating Manual, (2006-2007), pp. 117-145.
- 16 S.Y. Park, J.H. Kim, M.C. Kim, H.S. Song, C.G. Park, "Microscopic observation of degradation behavior in yttria and ceria stabilized zirconia thermal barrier coatings under hot corrosion Surface and Coatings Technology, 190, 2005, 357-365.
- 17 Saremi Mohsen, Afrasiabi Abbas, Kobayashi Akira, Bond coat oxidation and hot corrosion behavior of plasma sprayed YSZ coating on Ni superalloy, *Transactions of JWRI*, Vol. 36, 2007, No.1.
18. Sudhangshu Bose, High Temperature Coatings, Butterwoth-Heinmann, Elsevier Inc. 2007.
- 19 R. L. Jones, "Some aspects of the hot corrosion of thermal barrier coatings, Journal of Thermal Spray Coatings", Volume 6 (1), March 1997, 77-84.
- 20 N. Eliaz, G. Shemesh R. M. Latanision, "Hot corrosion in gas turbine components, Engineering Failure Analysis" (2002), 31-43.
- 21 W. O. Soboyejo, P. Mensah, R. Diwan, J. Crowe, S. Akwaboa, "High Temperature Oxidation interfacial Growth Kinetics in YSZ Thermal Barrier Coatings with Bond Coatings of NiCoCrAlY with 0.25% Hf", Journal Article, Materials Science and Engineering A 528 (2011) 2223-2230.
- 22 Stephen Akwaboa, Monica B. Silva, Patrick Mensah, Ravinder Diwan, Douglas E. Wolfe, and Shengmin Guo, "Comparison of Cyclic Oxidation Performance of APS and EBPVD Processed TBCs On IN 738 with a Bond Coat of NiCoCrAlY Powder with 0.25% Hf", Proceedings of the ASME 2009 International Mechanical Engineering Congress & Exposition, November 13-19, 2009, IMECE 2009-11901.
- 23 Ogad Agu, Ravinder Diwan, Patrick F. Mensah, Monica B. Silva, and S.M. Guo, "Porosity and Thermal Cycling Behavior of Plasma Sprayed and EBPVD Thermal Barrier Coatings", Proceedings of ASME Turbo Expo 2010: Power for Land, Sea and Air GT June 14-18, 2010, GT 2010- 22433.
- 24 M. Madhwal, E.H. Jordan, M. Gell, Mater. Sci. Eng. A384 (2004) 151–161.
- 25 E.Tzimas, H.Mullejans, S.D.Peteves, J.Bressers and W.Stamm, "Failures of Thermal Barrier Coating System under cyclic Thermo mechanical loading, Acta. mater Vol 48 (2000) 4699-4707
- 26 Bartlett, A. and Dal MASchio, R. J Am. Ceram Soc. , 1995, **78**(4), 11018
- 27 Haynes J.A., Ferber, M K., Porter, W.D and Rigney, E.D. Oxid. Metals, 1999, **52**(1/2), 31
- 28 DeMasi-Marcin, J.T., Sheffler, K.D and Bose, S. J. Eng. Gas Turbines Power, 1990, 112, 521.
- 29 Nissley, D.M., 1997, "Thermal Barrier Coating Life Modeling in Aircraft Gas Turbine. Engines," J. Thermal Spray Technol., Vol. 6(1), pp. 91-98

- 30 Qian, G., Nakamura, T., Berned, C.C and Leigh, S.H. *Acta mater.*, 1997, **45**(4), 1767.
- 31 Newaz, G.M., Nusier, S.Q and Chaudhury, Z. A. *J. Eng Mater. Tech.*, 1998, **120**, 149
- 32 Cheng, J., Jordan, E. H Barber, B. and Gell, M. *Acta mater.*, 1998, **46** (16), 5839.
- 33 Sergio, V and Clarke, D.R. *J. Am Ceram Soc.*, 1998, **81** (1203237).
- 34 Tuncer, O., Acharya, S., and Uhm, J., Hydrogen-Enriched Confined Methane Flame Behavior and Flashback Modeling, 44<sup>th</sup> AIAA Aerospace Sciences Meeting and Exhibit, Reno, Hanuary 2006, Paper Number AiAA-2006-754
- 35 Stephen Akwaboa and Patrick F. Mensah, “Effects of Thermal Radiation on Air Plasma Spray (APS) Coated Gas Turbine Blade”, Proceedings of 14th International Heat Transfer Conference IHTC14 -22961, August 8-13, 2010, Washington DC, USA